A Survey of Changes in Grasslands within the Tonle Sap Lake Landscape: 2004–2023

Monysocheata Chea , Benjamin T. Fraser * , Sonsak Nay , Lyan Sok , Hillary Strasser , Rob Tizard

Posted Date: 2 July 2024

doi: 10.20944/preprints202407.0174.v1

Keywords: Grasslands; Tonle Sap Lake; Land Use and Land Cover; Land Cover Change; Protected Areas; Google Earth Engine; Agriculture Expansion

Article

A Survey of Changes in Grasslands within the Tonle Sap Lake Landscape: 2004-2023

Monysocheata Chea [1,‡], Benjamin T. Fraser [2,‡,*], Sonsak Nay [1], Lyan Sok [1], Hillary Strasser [1] and Rob Tizard [1]

[1] Wildlife Conservation Society, Cambodia Program
[2] Department of Natural Resources and the Environment, University of New Hampshire
* Correspondence: Benjamin.fraser@unh.edu
‡ Indicates that authors have contributed equally to this manuscript.

Abstract: The Tonle Sap Lake (TSL) landscape is a region of vast natural resources and biological diversity in the heart of Southeast Asia. In addition to serving as the foundation for a highly productive fisheries system, this landscape is home to numerous globally threatened species. Despite recognition by several governmental and international agencies for decades, nine protected areas have been established within this region, natural landcover such as grasslands have experienced considerable declines since the turn of the century. This project used local expert knowledge to train and validate a random forest supervised classification of Landsat satellite imagery in Google Earth Engine. The time series of thematic maps was then used to quantify the conversion of grasslands to croplands between 2004 and 2023. The classification encompassed a 10-kilometer buffer surrounding the landscape, an area of nearly 3 million hectares. The average overall accuracy for these thematic maps was 82.5% (78.5%–87.9%), with grasslands averaging a 76.1% user's accuracy. The change detection indicated that over 207,281 ha of grasslands were lost over this period (> 59.5% of the 2004 area), with approx. 89.3% of this loss could be attributed to cropland expansion. The results of this project will inform conservation efforts focused on local scale planning and management of commercial agriculture.

Keywords: Grasslands; Tonle Sap Lake; Land Use and Land Cover; Land Cover Change; Protected Areas; Google Earth Engine; Agriculture Expansion

1. Introduction

The Tonle Sap Lake (TSL) floodplains and surrounding landscape are a region globally recognized for biodiversity and natural productivity [1–4]. Millions of people throughout the Lower Mekong River Basin rely on the TSL fisheries, water resources, and natural vegetation for their livelihoods [5,6]. Recognizing the importance of this landscape, UNESCO created the Tonle Sap Biosphere Reserve (TSBR) in 1997 which was further established by governmental royal decree in 2001 [3,5,7]. The TSBR is a major breeding area for at least a dozen globally threatened bird species [3,6,7]. These include the Lesser Adjutant (*Leptoptilos javanicus*), Painted Stork (*Mycteria leucocephala*), Asian Openbill (*Anastomus oscitans*), Black-headed Ibis (*Threskiornis melanocephalus*), Oriental Darter (*Anhinga melanogaster*), Sarus Crane (*Grus antigone*), and Bengal Florican (*Houbaropsis bengalensis*). These bird species, along with several environmental functions of this flood pulse ecosystem, are dependent on the mosaic of grasslands and other vegetation found throughout the floodplains. Despite the efforts of the Cambodian Ministry of Environment (MoE) and agencies such as the Wildlife Conservation Society (WCS) or BirdLife International this landscape and its grasslands are facing ongoing degradation due to commercial agricultural development [5,7–10]. Agricultural development threatens countless species, with the true extent of these impacts being uncertain due to limited ecosystem assessments.

Grasslands throughout the TSL landscape provide a variety of ecosystem services. Among these services are carbon storage and sequestration [11–13], water nutrient regulation, livestock food provisioning [14], and serving as wildlife breeding grounds and habitat [2,3,9,13]. Long term

 doi:10.20944/preprints202407.0174.v1

conservation efforts for these grasslands across the protected landscapes are aimed at the unique and globally threatened community of bird species found there. Historically, information on these bird populations have been gathered through assessments, made from field surveys, such as those documented by Seng et al., [15], van Zalinge [16], or Packman [6]. These surveys, however, are resource intensive and lack the ability to provide comprehensive information of the landscape on a time scale relevant to management action. Jointly, monitoring the expansion of croplands, such as rice, into these land cover could lead to vast increases in knowledge of the regional environmental status, food security and local socioeconomics [17,18]. The integration of remote sensing tools and geographic information systems (GIS) could lessen the resource requirements for conducting such surveys while at the same time providing accurate and up-to-date information on land cover dynamics.

The use of remote sensing for earth observation (EO) has expanded in recent decades to become an established and increasingly impactful method for obtaining information on land cover and land use (LCLU) [6,19–21]. Land cover acts as a key component for environmental monitoring and modelling for many projects [19,22,23]. Time series data, from programs such as Landsat, support landscape level analyses of land cover which would be cost prohibitive if conducted in the field (i.e., *in situ*). A widely used application of the land cover products derived from remotely sensed imagery are LCLU change detections [19,24,25]. Change detections provide crucial, site-specific information on the spatial distribution and abundance of land cover classes over time [21,26,27]. Such information can then be used to track the impacts of human development (such as cropland expansion), social pressures, or policy decisions by a wide range of stakeholders [28]. While these methods are increasingly available, they have not been applied ubiquitously [1]. Grasslands historically have been underrepresented in remote sensing analyses [6,12]. Few studies published over the last 20 years for this region specifically have reflected on changes in grassland abundance or distribution, which is a vital component for accurate and timely conservation action [9,24]. Sourn et al., [29] demonstrated a large change from forests to croplands in the nearby Battambang province between 1998 and 2018. The authors noted drives of this deforestation were likely policy, legal frameworks, and socio-economic pressures [29]. Mahood et al., [13] detailed that rice cultivation was likely the cause of substantial grassland and shrubland loss between 1993 and 2018 within the TSL and surrounding floodplains. Other studies of the early 2000's also portrayed large amounts of cropland expansion at the cost of natural vegetation cover throughout this region [5,10,30]. Conservation organizations working in the TSL landscape are facing limited resources and knowledge from which to base their decisions, due to the age of their data on remanent grasslands patches [2,4]. Measuring the current area and distribution of natural land cover types would aid management of this ecosystem [2]. Our study aims to inform local conservation efforts as well as provide an analytical framework for similar investigations of natural vegetation loss in neighboring regions. This research focuses on the full TSL landscape, including a 10km buffer from the WCS defined landscape ('stronghold') boundary. Within this area are nine protected areas, which face ongoing influence from a wide range of stakeholders [1,5,31,32]. This research also specifically addresses the losses of dry grasslands, which are a critical component of the local ecology. For these reasons, our objectives are to quantify losses in grasslands within the TSL landscape since the early 2000s. More specifically, this research aims to:

1. Quantify trends in land cover change, leading to losses in grasslands throughout the Tonle Sap Lake (TSL) landscape.

   Evaluate these changes in the context of dry grasslands, a vital wildlife habitat within this region.

   This analysis will help conservation efforts to specifically address losses at the landscape and key protected area scales.

2. Materials and Methods

2.1. Study Area

Preprints.org (www.preprints.org) | NOT PEER-REVIEWED | Posted: 2 July 2024 doi:10.20944/preprints202407.0174.v1

The TSL and surrounding floodplains are a key component of the Lower Mekong River Basin [1,13]. The core area is defined by the TSBR, which is designated for protecting biodiversity, limiting habitat disturbance, and serving as a site for research [7,13]. The area of open water within this flood pulse system has been measured to expand as much as five times between the dry and wet seasons [3]. Intermixed with the flooded forests, spreading outwards from the open waters are a mosaic of grassland patches and scrub/shrublands [3,4,7], leading into croplands. To ensure that the entire landscape is considered in this analysis, a 10 km buffer was applied to the TSBR extent (Figure 1). This 2.99-million-hectare (ha) area, in black, represents the primary extent for this analysis.

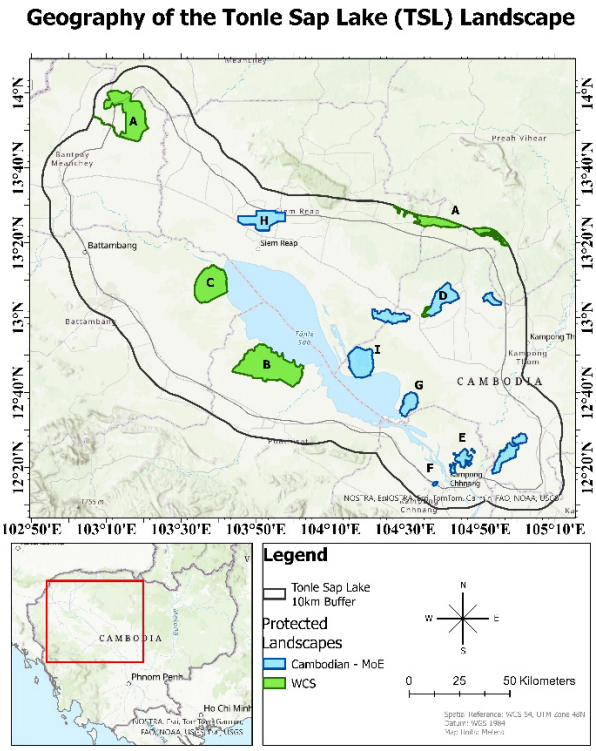

Figure 1. Tonle Sap Lake (TSL) landscape and protected areas. Protected areas include: A—Ang Trapeng Thmor, B—Bakan, C—Prek Toal, D—Kampong Thom, E—Phnom Neang Kong Rey- Phnom Touk Meas, F—Phnom Krang Dey Meas, G—Stung Sen Core Area (Ramsar Site), H—Angkor, I—Boeng Chhmar Core Area (Ramsar Site). Those given in blue are regulated by the Royal Cambodian Government (RCG) Ministry of Environment (MoE). Those given in green are monitored and manged by the Wildlife Conservation Society (WCS).

Nine protected areas are located throughout the TSBR (Figure 2). These protected areas make up approximately 170,056 ha within the study region (~5% of the total area) [33]. The protected areas range in size from 288 ha (Phnom Krang Dey Meas) to over 38,000 ha (Bakan). These areas have each been established for the conservation of critically endangered species, such as the Bengal Florican, Sarus Crane, or the vulnerable Manchurian Reed Warbler (*Acrocephalus tangorum*) [9,34,35]. The updated boundary files for these protected landscapes were downloaded from Protected Planet [33].

 doi:10.20944/preprints202407.0174.v1

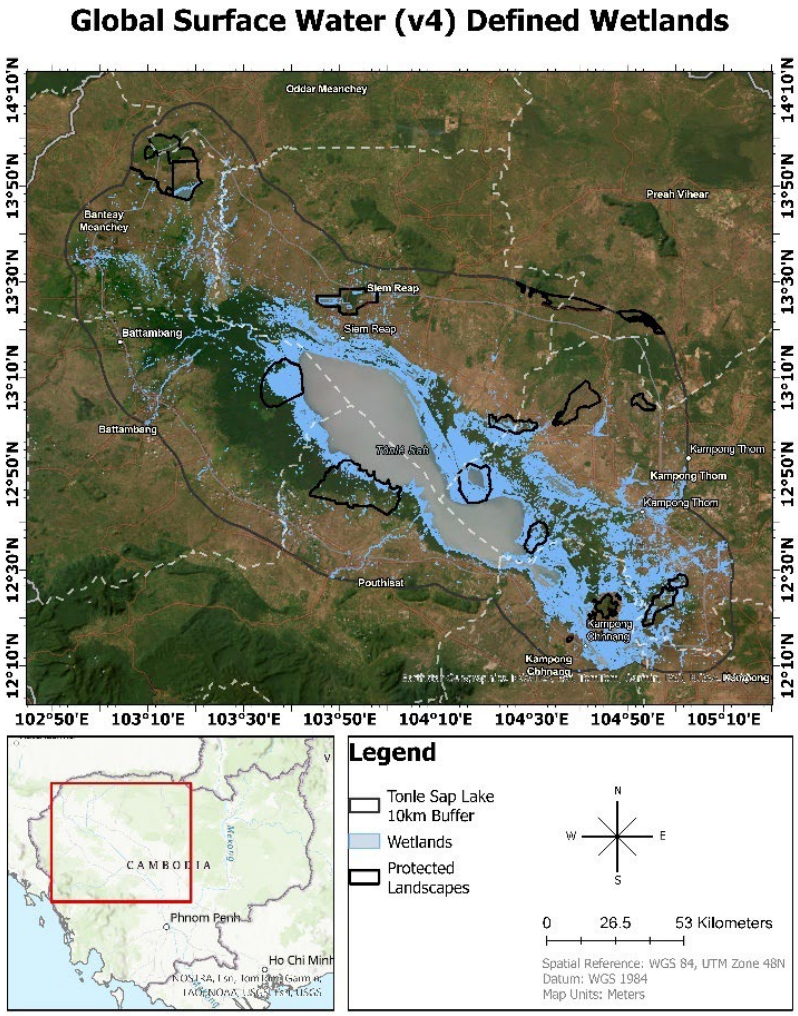

Figure 2. European Union (EU) Joint Research Centre (JRC) surface water occurrence ≥ 20% layer used to define corresponding grassland areas as wet grasslands. Grassland areas located outside of this polygon were defined as dry grasslands.

2.2. Satellite Imagery

A combination of Landsat 5 Thematic Mapper (TM) and Landsat 8 Operational Land Imager (OLI) Level 2 (surface reflectance corrected) imagery were used to generate landcover maps of this region throughout the study period. Landsat images are widely established for land cover mapping and time series analyses, even for grassland areas [11,14,19,28]. Google Earth Engine (GEE) (Mountain View CA, USA) was used to compile Landsat imagery and perform the classification. This cloud-based GIS greatly reduced the burden of computational complexity for this analysis [18,28,36]. Imagery were queried of the dry seasons from 2004, 2008, 2013, 2018, and 2023. Dry season imagery were defined as those taken between November of the previous year and early April of the defined year. For example, the 2004 dry season would be defined as November 1st, 2003 through April 1st, 2004. This period was selectively sampled due to the consistent cloud and shadow coverage throughout the rest of the year [29]. A more consistent 5-year time step was desired for this analysis, however, imagery from the 2003 dry season were of poor quality and considerable cloud coverage.

For each of the five years mapped in this study, the image collections were comprised of roughly 30-40 individual Landsat images (i.e., scenes). A pixel-based composite was made from each collection of images. These composites are a common technique for creating a singular image, with reduced noise, across the study region from which image analysis and classification could be performed [19,37–40]. The specific technique for creating these composites was based on the median

 doi:10.20944/preprints202407.0174.v1

pixel algorithm. This algorithm finds the median value for each band across an image stack and has been found to generate a more radiometrically consistent result [41–43].

2.3. Reference Data

Three sources of reference data were used to support the training and validation of the 2004, 2008, 2014, 2018, and 2023 thematic maps. These sources of reference data were integrated because they most closely matched the land cover dynamics of the studied years, were based on reliable methods, and ensured that the earliest maps (2004 and 2008) were comparable to historic surveys of grasslands within this geography. First, historic habitat data from the early 2000's was used to guide the 2004 and 2008 classifications. This habitat data consisted of 1,250 grassland samples, 1,240 shrubland/forest samples, and 780 cropland samples generated through the interpretation of high-resolution imagery [44]. These data were also used to established estimates of grassland habitat by earlier surveys [6]. Second, the WCS Cambodia GIS team provided maps of the landscape digitized from high-resolution 2021 and 2022 imagery. These maps were used to generate samples from homogeneous areas of shrublands (n = 1,200), forests (n = 700), grasslands (n = 1,200), and rice croplands (n = 1,000). These samples were used to guide the classification of the 2014, 2018, and 2023 imagery. Lastly, the WCS Cambodia team independently conducgted an analysis of change in grasslands within the Bakan and Ang Trapeng Thmor (ATT) protected areas. From this analysis, 75 reference samples per class were integrated into the classification of the larger landscape. Samples for the class 'water' were generated through interpretation of both the high-resolution basemap imagery and the respective Landsat composite.

The previously established sources of reference data were used by a trained image interpreter as a guide for manually entering reference samples using the GEE geometry tools. For each of the five classifications, 600 to 800 reference samples were entered. These samples were geographically distributed, with a minimum of 100 samples per class per map, and were based on a higher level of detail than the Landsat imagery provided [27,45].

2.4. Land Cover Classes

Land cover classes within the TSL landscape were distinguished based on definitions adapted from the European Space Agency (ESA) WorldCover project classification scheme [46]. The classes defined here included grasslands, forest/shrub, croplands, water, and village/road. The full definition for each class is provided below in Table 1. Additional attention was given when defining the characteristics of grasslands, croplands, and village/road classes due to their influence on the analysis. The definition for grasslands, which is also consistent with Sourn et al., [29], is marked by the absence (minimal coverage) of trees or shrubs [12]. Croplands were understood to be one of the most abundant land cover types throughout Cambodia [31]. While many crop types could exist within this region, previous studies reported that paddy rice make up more than 70% of the croplands within the TSL floodplains [13,31]. Lastly, village/road was important to distinguish due to its considerable distribution throughout the study region. The scattered buildings and unpaved roads however were difficult to distinguish from barren areas or dry season croplands due to the limited spatial resolution found with the Landsat imagery [47]. For this reason, we used a Cambodia roads layer (updated in 2013) as a mask to serve as these areas, rather than including this class within the supervised classification [48]. The roads layer lines were buffered 10 meters (m) to cover the average road diameter. The roads layer mask was integrated after the GEE classification.

Table 1. Land cover class definitions. Adapted from European Space Agency (ESA) WorldCover project classification scheme [46].

Land Cover Class	Definition
Grasslands	Any area dominated by > 10% herbaceous plants (i.e., those with a persistent stem but lacking woody/firm structure). These may include grasslands, prairies, pastures, or savannahs. Woody plants, such as

 doi:10.20944/preprints202407.0174.v1

	trees and shrubs may be present with coverages < 10%. Abandoned croplands are also included in the class if herbaceous coverage is > 10%.
Forest/Shrub	Any area dominated by trees or shrubs with a combined coverage > 10%. Other land cover classes such as grasslands, croplands, or water may be present beneath the tree canopy. Areas planted for commercial agriculture (including rubber plantations) are not included in this class. This class does include seasonally flooded areas.
Croplands	Any area covered by planted/sowed crops. These croplands may consist of herbaceous or woody crops including paddy rice, rubber, cashew, cassava, or a mixture of other crops. Croplands may be irrigated or rainfed within this region.
Water	Any area dominated by open water during the majority of the dry and wet seasons. These may include lakes, reservoirs, or rivers.
Village/Road	Any area covered by buildings, roads, or other artificial (i.e., built-up) structures.

To further define dry from wet grassland communities across the floodplains, the European Union Joint Research Centre (JRC) Global Surface Water layer (v4) was used [49]. Specifically, the (monthly) occurrence frequency estimated from 1984–2021 surface water presence was used to define a threshold between these vegetation communities. An occurrence value greater than or equal to 20% (≥ 20%) defined wetland areas (Figure 2). Grassland areas outside of this polygon were defined as dry grasslands.

2.5. Land Cover Classification and Change Analysis

The image mosaics for the full study region, Bakan, and ATT were independently classified in GEE using a random forest supervised classification [14,50]. These classifications resulted in three separate land cover maps for 2004, 2008, 2014, 2018, and 2023. The random forest algorithm, like other machine learning methods, is documented to handle complex classes and high dimensionality of input data better than conventional classifiers [19,51]. The random forest algorithm is also commonly used for paddy rice mapping which is known to be in high abundance throughout this region [17]. In addition to the original Landsat bands, seven spectral indices and Shuttle Radar Topography Mission (SRTM) slope data were used in the classification [52]. The goal of this combination of data was to maximize the spectral uniqueness of each land cover class [20,21,36]. The spectral indices included: Normalized Difference Vegetation Index (NDVI) [12,21,53], Soil Adjusted Vegetation Index (SAVI) [14,54], Enhanced Vegetation Index (EVI) [36,53], Greenness Index (GI), Moisture Stress Index (MSI) [55], Normalized Difference Water Index (NDWI) [55], and Normalized Burn Ratio (NBR) [56,57]. The SRTM elevation layer was used to improve the differentiation of flat croplands and upland forests [52,58].

Several hyperparameters of the random forest classification algorithm were tuned during initial testing of the results. These hyperparameters included the number of decision trees, the proportion of training and validation data, and the total selection of input features. The number of decision trees was kept at 500, which is documented to be a basic minimum for increasing the consistency of the results [50]. The reference data were split with a random 55% of the samples per class being used for training and 45% being used for validation (i.e., testing). These proportions ensured that a minimum valid sample size for each class was available for independently conducting the accuracy assessments [45]. Lastly, the selection of input features was determined through a relative feature importance calculation [36,59]. The feature importance test. The results of the relative feature importance test, in

 doi:10.20944/preprints202407.0174.v1

combination with the impacts on the overall accuracy when removing specific features, were used to achieve the best classification performance [36,60–62].

Following the land cover classifications in GEE, each map was exported using Google Drive and opened using ArcGIS Pro (v3.1, Redlands CA, USA). Minor editing of misclassified areas was performed on each map by local experts to improve the quality of the results and subsequent change detection analysis [27]. The maps were converted to shapefiles to perform these edits. These edits included first running the eliminate tool on each map. The eliminate tool was used to dissolve any isolated singular pixel sized polygon into the neighboring polygon of the largest size. For example, isolated polygons less than 0.02 ha in size classified as water but located in the middle of a large cropland area were dissolved into the surrounding croplands. Running the eliminate tool reduced the noise commonly found when using pixel-based classifications [63,64]. Secondly, while reviewing the land cover maps, minor manual revisions were made when areas were recognized as being misclassified and the correct class could be confirmed by a combination of interpretation of the corresponding image mosaic and available reference data.

The final land cover maps for each of the three sites were then merged and used to conduct a post-classification change detection. Post classification change detections have historically been among the most applied change detection methods, providing a straightforward approach to changes over time [24,26,53]. The ArcGIS Pro categorical change detection tool ('compute change detection') was used so that the spatial distribution and specific types of categorical change could be evaluated [21,24]. We specifically selected changes from grasslands to croplands for each of the four time steps: (1) 2004 to 2008, (2) 2008 to 2014, (3) 2014 to 2018, and (4) 2018 to 2023. Changes from forest/shrub to croplands were independently assessed to compare our models results with those of previous studies [5,13].

2.6. Accuracy Assessment

The accuracy of each land cover map was independently assessed in GEE using a thematic map accuracy assessment error matrix [45,65]. In total, 15 error matrices were produced, which provided quantifications of the overall accuracy (OA), producer's accuracy (PA), and user's accuracy (UA) for each map. The final map depicting changes from grasslands to croplands over time (2004 to 2023) was assessed using a change detection error matrix calculated from an ArcGIS Pro accuracy assessment [24,26,45,66,67]. For this assessment, there was one 'change' class ('grasslands to croplands') and two 'no change' classes ('grasslands' and 'croplands'). One hundred samples were randomly distributed within each strata (i.e., class) to perform this assessment. The validation of these samples was performed using through the 2004 Landsat image mosaic, 2023 Landsat image mosaic, and ArcGIS Pro high-resolution basemap imagery for image interpretation.

The map and accuracy assessment produced from the change detection analysis were also subsequently evaluated based on the recommendations of Olofsson et al. [27,68]. Using the sample-based accuracy assessment performed in ArcGIS Pro, the area-weighted accuracy and uncertainty were used to generate an area-based error matrix and corresponding confidence intervals for an adjusted estimate for the amount of changed and unchanged area. Confidence intervals (95%) were calculated for these adjusted areas [27,68].

3. Results

3.1. Land Cover Classification and Change Detection Analysis

The five thematic maps produced for the full study region achieved an average overall accuracy of 83.5%. The average class-specific user's accuracies were 88.5% for forests, 76.1% for grasslands, 82.5% for croplands, and 90.8% for water. The overall accuracy, user's accuracy (UA), and producer's accuracy (PA) for the primary classes of interest (grasslands and croplands) are reported in Table 2. Confusion between the forest and croplands classes outside of the floodplain decreased the accuracy for both classes for the 2023 classification.

 doi:10.20944/preprints202407.0174.v1

Table 2. Accuracy for mapping grasslands and croplands throughout the TSL landscape for each of the five thematic maps. Reported are the overall accuracy of the maps, the user's accuracy (UA), and the producer's accuracy (PA) for the grasslands and croplands classes.

	2004	2008	2014	2018	2023
Overall Accuracy	88.5%	86.7%	87.9%	78.5%	79.8%
Grasslands UA	84.6%	88.2%	78%	84.6%	90%
Grasslands PA	83.9%	68.2%	72.2%	59.5%	78.3%
Croplands UA	92.2%	71.9%	93.3%	84.6%	31.7%
Croplands PA	87.7%	86.8%	87.4%	84.6%	48.1%

The change detection analysis reported that throughout the 2004 to 2023 study period, a total of 207,281.4 ha of grasslands (*both wet and dry types*) were lost. This loss reflects a 59.5% decrease in grassland area since 2004 (approximately 3.13% annual decline). This rate, however, was not consistent. Between 2014 and 2018 the rate of decline was 6.7%, while between 2008 and 2014 the rate of decline was 22.0%. The average 4-to-5-year loss was 14.9%.

In 2004, the dry grasslands represented 297,004.7 ha out of the 348,300 ha of total grasslands present within the study area (85.3% of the total area). The estimated loss of dry grasslands over the study period was 174,400.2 ha (Figure 3). This is an estimated decline in area of 58.7% since 2004, a rate of 3.09% annually (Table 3).

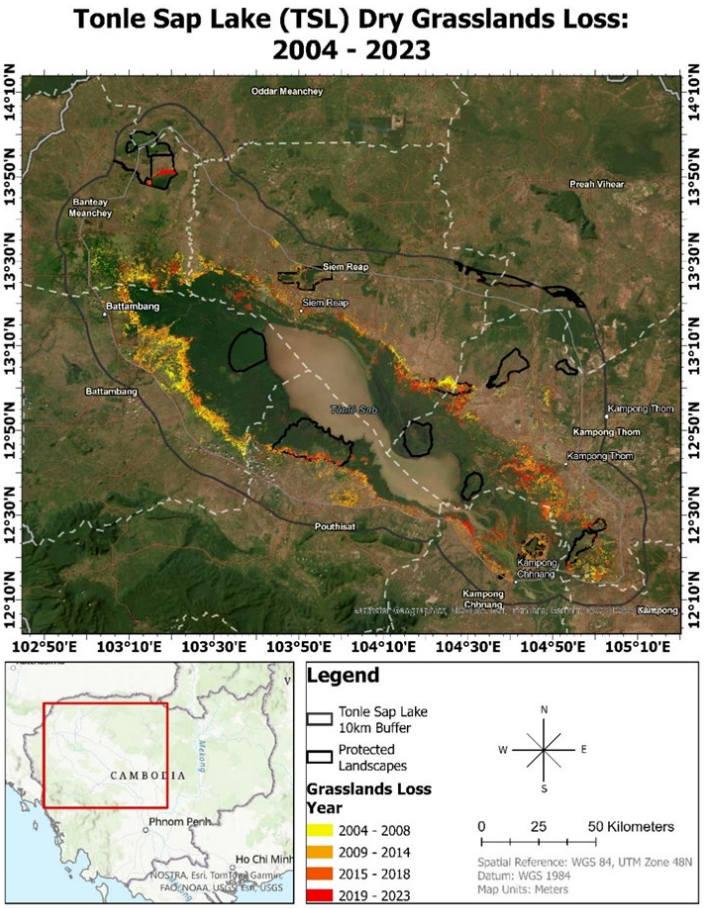

Figure 3. Grasslands loss (dry only) between 2004 and 2023. Grasslands loss is symbolized based on four distinct time periods: yellow (grasslands lost between 2004 and 2008), orange (2009-2014 losses), dark orange (2015-2018), and red (2019-present).

 doi:10.20944/preprints202407.0174.v1

Table 3. Annual grassland cover estimates for the study area based on the classified land cover maps.

Dry Grasslands Loss		
Year	**Hectares**	**Percent decrease**
2004	297,004.71	Baseline
2008	253,596.98	15%
2014	192,452.50	20.59%
2018	171,072.58	7.20%
2023	122,604.53	16.32%
Total Decrease (2004-2023)	**174,400.18**	**58.7%**

Within the nine protected areas, the cropland area increased by 37.1% over the study period (approx. 36,400 ha to 49,900 ha). Dry grasslands within these same areas experienced a decline in area of 45.4% between 2004 and 2023. Within the largest protected area, Bakan, the estimated loss of dry grassland was 26.6% (approx. 2,806.1 ha of the of the 10,531.7 ha of dry grasslands present in 2004). This same protected area experienced an increase in cropland land cover of 137.3% since 2004.

The total increase in cropland land cover within the study region was 347,059 ha, a 27.3% increase in area since 2004. The increase in cropland area accounts for 55.7% of the losses in natural vegetation (grasslands, forests, and shrubs) from 2004 to 2023. For the dry grasslands specifically, 89.3% of the decline in land area can be accounted for by expansions in croplands (155,725.8 ha of the total 174,400.18 loss).

3.2. Accuracy Assessment

An area-weighted and error adjusted assessment of the change detection analysis is reported in Table 4. This analysis of error and uncertainty for the change (dry grasslands converted to croplands) and no change (unchanged dry grasslands and unchanged croplands) classes shows that the total amount of grasslands lost between 2004 and 2023 as reported by the maps may be underrepresented. Instead of 174,400 ha of loss, the error-adjusted area depicts a total loss of 216,965.7 ha of loss (24.4% higher estimate). The 95% confidence interval for this estimated loss is 196,900 ha to 237,100 ha (216,965.7 ha ± 20,103 ha). This area-based accuracy assessment achieved an overall accuracy of 82.89%.

Table 4. Area-weighted accuracy assessment and error adjusted land cover area estimates for the change detection analysis based on Olofsson et al., [27,68].

Class	Map Area (hectares)	Adjusted Area (hectares)	95% CI (hectares)	User's Accuracy	Producer's Accuracy	Overall Accuracy
Change	174,400.18	216,965.70	20,102.80	69.0%	55.5%	**83.89 %**
Dry Grasslands	122,604.53	248,575.82	18,989.90	64.0%	31.6%	
Croplands	1,618,810.00	1,450,273.18	18,308.45	87.0%	97.1%	

4. Discussion

The results of this analysis, like earlier studies, demonstrate a drastic decline in natural landcover throughout the TSL landscape due to cropland expansion. Kummu et al., [2] made a call

 doi:10.20944/preprints202407.0174.v1

for improving knowledge of this ecosystem, through surveys of the natural land cover types and resources nearly 20 years ago, yet such knowledge is still critically limited. Reliable information specifically on grassland ecosystems, such as their distribution and quality is important for successful conservation [6,14,36]. To address the study objectives and support the management of critically endangered wildlife habitat within the TSL landscape, losses of both grassland and dry grassland were evaluated between 2004 and 2023. The post-classification change detection analysis reported declines in grasslands and dry grassland of 207,281 ha (59.5%) and 174,400.2 ha (58.7%) respectively. The five thematic maps used for this analysis, which achieved an average overall accuracy of 83.5%, depicted a 3.09% annual decline in dry grassland area. A quantification of the area-weighted and error-adjusted change detection analysis reports that the actual decline in dry grassland area would be closer to 216,965.7 ha. The 95% confidence interval on this calculation shows a decline of 66% to 80% between 2004 and 2023 [27,68]. Within the nine protected areas, 45.4% of the dry grasslands were lost between 2004 and 2023. Based on these estimates, the 5% of land currently designated as protected areas within this region showed a 13.3% lower decline in dry grasslands than the study area average. This 13.3% lower rate of decline is notable but demonstrates that further conservation action is needed within the TSL landscape, even within the protected areas.

The loss of grasslands, especially tropical grasslands is substantial across Southeast Asia, and represents the loss of a highly valuable ecosystem [6]. Land cover change has a long-recognized influence on ecological systems [27,69,70]. Packman et al. [10] predicted in 2014 that if rates of grassland decline (habitat loss) for the Bengal Florican continued for the following decade (2012-2022) then the critically endangered Bustard would become extinct. Our estimate show that 122,604 ha (41.3%) of the 2004 grassland area still remains within this landscape. This estimate, however, does not take into account the number of patches meeting the minimum habitat requirement for this species. Studies by Niu et al., [31] and Senevirathne et al., [30] marked historic trends in the expansion of agriculture. In agreement with these findings, this study estimates an increase in cropland area of 27.3% (347,059 ha) within the TSL landscape. Chen et al., [5] found a substantial decline in forest cover in their study of the TSL landscape between 1992 and 2019 (2.3% annual decline). Our analysis of the 2004 to 2023 forest cover trends found identical rates of decline for this land cover class (2.3% annually). Regarding the influence of croplands on the loss of grasslands, Packman et al., [6,10,71] quantified that 95% of the grassland losses in the south-eastern region of the Tonle Sap floodplain were attributable to rice cultivation. Our analysis across the entire landscape suggests that 89.3% of the loss in dry grasslands can be accounted for by increases in cropland area. The difference in these estimates could be contributed to either the differences in study area or the differences in the definition of grasslands. The 2011 study defined grasslands based on soil types while this study used the frequency of water occurrence [6].

The use of machine learning classification and regression methods for grasslands monitoring is increasing yet still underrepresented in current remote sensing applications [12,14]. Like other studies investigating complex land cover and land use change dynamics over large areas, this project faced several challenges. First, change detections accuracy assessments are particularly difficult due to the availability and reliability of historic reference data, especially over large areas [19,24,53]. This study relied on reference data generated from the interpretation of historic and more recent high-resolution imagery. While a large number of reference data samples for each land cover class were generated, they were not specific to each of the five years classified during this study. Compounding the challenge of adapting the available reference data to this study was the diverse mixture of vegetation found within the floodplains. Image analysis of areas with diverse vegetation mixtures can be difficult with moderate resolution imagery such as Landsat [20]. The flooded forests, shrublands, and grasslands in many areas are a patchwork mosaic of emergent vegetation [3]. Due to this challenge, reference samples with limited certainty when compared to the Landsat image mosaics were removed from the analysis. A second potential source of uncertainty in this analysis was the use of a post-classification change detection. No single change detection method can be optimal for all cases [19,24,53]. This study used the given approach due to its ease of implementation and established reliability [24,26,53]. Future studies should leverage the potential of more advanced

 doi:10.20944/preprints202407.0174.v1

land cover trend analyses such as Continuous Change Detection and Classification (CCDC) or LandTrendr to generate more precise estimates of land cover change [72–76]. Lastly, the classifications in this study relied on a combination of optical imagery and elevation data. While Landsat imagery provided a stable data source, optical imagery collections for each mapping period were limited in this region to only the dry seasons [14,18,28]. Imagery queried from May to October of each year contained considerable amounts of clouds, shadows, and noise, degrading the quality of the median pixel mosaics. The obstruction of clouds throughout the wet season also meant that seasonal image composites, a stack containing bands from two or more seasons within a year, were unfeasible [21,37,77,78]. A combination of optical and Synthetic Aperture Radar (SAR) remotely sensed data has shown promise in paddy rice mapping, due to the change in growth stage across seasons, but was not approached in this study [17,18]. A supplemental goal of this analysis was to provide a methodology which could be easily trained and adapted to neighboring regions.

The results of this study are not unique to the TSL landscape and should be used to inform broader conservation policy and monitoring efforts. Agricultural expansion into areas of natural vegetation are a global issue [29]. Rice cultivation has existed in this region for over 1,000 years [9]. It has only been for the last 20 to 30 years that industrial-scale rice production has been a major threat to grasslands habitat [10]. The onset and escalation of this disturbance was caused by a mixture of social, economic, and political challenges [13]. Many of the villages within the TSL landscape are reliant on agriculture [79,80]. Studies have shown that simply increasing the land in production by each farmer does not cause a net increase in their income [80]. The rate of population growth, coupled with the high population density in the TSL landscape will further burden these efforts in the coming decades [4,5]. The results of this conflict between social and ecological needs will result in the further decline, and potential extinction, of grassland dependent species such as the Bengal florican [9,13]. To avoid this potential outcome, locally integrated conservation organizations must continue to increase their engagement with local farmers and commercial stakeholders [6,13,79]. Management decisions must also be supported and enriched by the most capable cloud computing and EO methods [36,81].

5. Conclusions

The Tonle Sap Lake (TSL) landscape supports a rich diversity habitat and ecosystem services utilized by over a million people in the Lower Mekong River Basin and numerous critically endangered species. To support the local biodiversity, nine protected areas totaling more than 170,000 ha have been established throughout this region. Despite the ongoing conservation efforts, historic studies and local experts have reported drastic declines in grasslands over the last two decades. This analysis surveyed land cover changes from 2004 to 2023 within the TSL landscape and surrounding 10km buffer area to generate current and reliable estimates of the declines in grasslands and dry grasslands. Five thematic maps, achieving an average overall accuracy of 83.5%, were used to perform a change detection analysis. From 2004 to 2023 the estimated decline in dry grasslands was 174,400.2 ha (58.7% of the area in 2004). Within the areas no longer containing dry grasslands, 89.3% were classified as croplands in 2023. An analysis of the protected landscapes estimated that 45.4% of the dry grasslands present in 2004 were lost by 2023. Future conservation efforts should build on the methods and results used here as a pathway to local scale management and outreach. Without an increase in current, reliable, and comprehensive data on the trends and distribution of land cover such as dry grasslands within this region, the conservation efforts aimed at protecting the numerous critically endangered and threatened species would be restricted in their potential.

Author Contributions: Conceptualization, B.T.F., H.S. and R.T.; Methodology, M.C., B.T.F., S.N., and L.S.; Validation, B.T.F. and M.C.; Resources, H.S., R.T., and B.F.; Data Curation, M.C., L.S., S.N., and B.T.F.; Writing—original draft preparation, B.T.F.; Review and Editing, H.S., R.T., M.C., S.N., and L.S.; Project Administration, H.S., R.T., and B.T.F.; Funding Acquisition, H.S. and R.T.

Funding: This research was partially funded by the Wildlife Conservation Society EU 'Our Tonle Sap Project' Grant # 111918, Reference Key 3: WCS 660.22.

Institutional Review Board Statement: NA

Data Availability Statement: Data is available by contacting Rob Tizard (rtizard@wcs.org)

Acknowledgments: NA

Conflicts of Interest: The authors declare no conflicts of interest.

References

1. Lamberts, D. The Tonle Sap Lake as a Productive Ecosystem. *Int J Water Resour Dev* 2006, *22*, 481–495.
2. Kummu, M.; Sarkkula, J.; Koponen, J.; Nikula, J. Ecosystem Management of the Tonle Sap Lake: An Integrated Modelling Approach. *Int J Water Resour Dev* **2006**, *22*, 497–519, doi:10.1080/07900620500482915.
3. Campbell, I.C.; Poole, C.; Giesen, W.; Valbo-Jorgensen, J. Species Diversity and Ecology of Tonle Sap Great Lake, Cambodia. *Aquat Sci* **2006**, *68*, 355–373, doi:10.1007/s00027-006-0855-0.
4. Uk, S.; Yoshimura, C.; Siev, S.; Try, S.; Yang, H.; Oeurng, C.; Li, S.; Hul, S. Tonle Sap Lake: Current Status and Important Research Directions for Environmental Management. *Lakes and Reservoirs: Science, Policy and Management for Sustainable Use* 2018, *23*, 177–189.
5. Chen, A.; Chen, A.; Varis, O.; Chen, D. Large Net Forest Loss in Cambodia's Tonle Sap Lake Protected Areas during 1992-2019. *Ambio* **2022**, *51*, 1889–1903, doi:10.1007/s13280.
6. Packman, C.E. Seasonal Landscape Use and Conservation of a Critically Endangered Bustard: Bengal Florican in Cambodia. Doctor of Philosophy, University of East Anglia, 2011.
7. Van Zalinge, R.; Evans, T.; Visal, S. A Review of the Status and Distribution of Large Waterbirds in the Tonle Sap Biosphere Reserve; 2008;
8. Gray, T.N.E.; Collar, N.J.; Davidson, P.J.A.; Dolman, P.M.; Evans, T.D.; Fox, H.N.; Chamnan, H.; Borey, R.; Kim Hout, S.; van Zalinge, R.N. Distribution, Status and Conservation of the Bengal Florican Houbaropsis Bengalensis in Cambodia. *Bird Conserv Int* **2009**, *19*, 1–14, doi:10.1017/S095927090800765X.
9. Mahood, S.P.; Hong, C.; Virak, S.; Sum, P.; Garnett, S.T. Catastrophic Ongoing Decline in Cambodia's Bengal Florican Houbaropsis Bengalensis Population. *Bird Conserv Int* **2019**, *30*, 1–15, doi:10.1017/S0959270919000157.
10. Packman, C.E.; Showler, D.A.; Collar, N.J.; Virak, S.; Mahood, S.P.; Handschuh, M.; Evans, T.D.; Chamnan, H.; Dolman, P.M. Rapid Decline of the Largest Remaining Population of Bengal Florican Houbaropsis Bengalensis and Recommendations for Its Conservation. *Bird Conserv Int* **2014**, *24*, 429–437, doi:10.1017/S0959270913000567.
11. Ali, I.; Cawkwell, F.; Dwyer, E.; Barrett, B.; Green, S. Satellite Remote Sensing of Grasslands: From Observation to Management. *Journal of Plant Ecology* **2016**, *9*, 649–671, doi:10.1093/jpe/rtw005.
12. Reinermann, S.; Asam, S.; Kuenzer, C. Remote Sensing of Grassland Production and Management-A Review. *Remote Sens (Basel)* 2020, *12*.
13. Mahood, S.P.; Poole, C.M.; Watson, J.E.M.; MacKenzie, R.A.; Sharma, S.; Garnett, S.T. Agricultural Intensification Is Causing Rapid Habitat Change in the Tonle Sap Floodplain, Cambodia. *Wetl Ecol Manag* **2020**, *28*, 713–726, doi:10.1007/s11273-020-09740-1.
14. Wang, Z.; Ma, Y.; Zhang, Y.; Shang, J. Review of Remote Sensing Applications in Grassland Monitoring. *Remote Sens (Basel)* 2022, *14*.
15. Seng, K.H.; Pech, B.; Poole, C.M.; Tordoff, A.W.; Davidson, P.; Delattre, E. *Directory of Important Bird Areas in Cambodia Key Sites for Conservation* ; 2002;
16. van Zalinge, R. AN ASSESSMENT OF EXOTIC SPECIES IN THE TONLE SAP BIOSPHERE RESERVE AND ASSOCIATED THREATS TO BIODIVERSITY A RESOURCE DOCUMENT FOR THE MANAGEMENT OF INVASIVE ALIEN SPECIES; 2006;
17. Zhao, R.; Li, Y.; Ma, M. Mapping Paddy Rice with Satellite Remote Sensing: A Review. *Sustainability (Switzerland)* 2021, *13*, 1–20.
18. Park, S.; Im, J.; Park, S.; Yoo, C.; Han, H.; Rhee, J. Classification and Mapping of Paddy Rice by Combining Landsat and SAR Time Series Data. *Remote Sens (Basel)* **2018**, *10*, doi:10.3390/rs10030447.
19. Gómez, C.; White, J.C.; Wulder, M.A. Optical Remotely Sensed Time Series Data for Land Cover Classification: A Review. *ISPRS Journal of Photogrammetry and Remote Sensing* 2016, *116*, 55–72.
20. Van Cleemput, E.; Adler, P.; Suding, K.N. Making Remote Sense of Biodiversity: What Grassland Characteristics Make Spectral Diversity a Good Proxy for Taxonomic Diversity? *Global Ecology and Biogeography* **2023**, *32*, 2177–2188, doi:10.1111/geb.13759.
21. Jensen, J. *Introductory Digital Image Processing: A Remote Sensing Perspective*; 4th editio.; Pearson Education Inc.: Glenview, IL, 2016;
22. Lambin, E.F.; Turner, B.L.; Geist, H.J.; Agbola, S.B.; Angelsen, A.; Folke, C.; Bruce, J.W.; Coomes, O.T.; Dirzo, R.; George, P.S.; et al. The Causes of Land-Use and Land-Cover Change : Moving beyond the Myths. **2001**, *11*, 261–269.

23. Hasan, S.; Shi, W.; Zhu, X. Impact of Land Use Land Cover Changes on Ecosystem Service Value - A Case Study of Guangdong, Hong Kong, and Macao in South China. *PLoS One* **2020**, *15*, 1–20, doi:10.1371/journal.pone.0231259.
24. Lu, D.; Mausel, P.; Brondízio, E.; Moran, E. Change Detection Techniques. *Int J Remote Sens* **2004**, *25*, 2365–2401, doi:10.1080/0143116031000139863.
25. Singh, A. Review Articlel: Digital Change Detection Techniques Using Remotely-Sensed Data. *Int J Remote Sens* **1989**, *10*, 989–1003, doi:10.1080/01431168908903939.
26. Macleod, R.D.; Congalton, R.G. A Quantitative Comparison of Change-Detection Algorithms for Monitoring Eelgrass from Remotely Sensed Data;
27. Olofsson, P.; Foody, G.M.; Herold, M.; Stehman, S. V.; Woodcock, C.E.; Wulder, M.A. Good Practices for Estimating Area and Assessing Accuracy of Land Change. *Remote Sens Environ* 2014, *148*, 42–57.
28. Hemati, M.; Hasanlou, M.; Mahdianpari, M.; Mohammadimanesh, F. A Systematic Review of Landsat Data for Change Detection Applications: 50 Years of Monitoring the Earth. *Remote Sens (Basel)* 2021, *13*.
29. Sourn, T.; Pok, S.; Chou, P.; Nut, N.; Theng, D.; Rath, P.; Reyes, M.R.; Prasad, P.V.V. Evaluation of Land Use and Land Cover Change and Its Drivers in Battambang Province, Cambodia from 1998 to 2018. *Sustainability (Switzerland)* **2021**, *13*, doi:10.3390/su132011170.
30. Senevirathne, N.; Mony, K.; Samarakoon, L.; Kumar, M.; 1c, H. *LAND USE/LAND COVER CHANGE DETECTION OF TONLE SAP WATERSHED, CAMBODIA*; 2010;
31. Niu, X.; Hu, Y.; Lei, Z.; Wang, H.; Zhang, Y.; Yan, H. Spatial and Temporal Evolution Characteristics of Land Use/Cover and Its Driving Factor in Cambodia during 2000–2020. *Land (Basel)* **2022**, *11*, doi:10.3390/land11091556.
32. Sok, S.; Chhinh, N.; Hor, S.; Nguonphan, P. Climate Change Impacts on Rice Cultivation: A Comparative Study of the Tonle Sap and Mekong River. *Sustainability (Switzerland)* **2021**, *13*, doi:10.3390/su13168979.
33. UNEP-WCMC; IUCN Protected Planet: The World Database on Protected Areas (WDPA) and World Database on Other Effective Area-Based Conservation Measures (WD-OECM) [Online].
34. Khmer Times Bakan Grassland Designated as Natural Protected Area.
35. Wildlife Conservation Society (WCS) Cambodia CONSERVATION AT ANG TRAPEANG THMOR Available online: https://cambodia.wcs.org/About-Us/Latest-.
36. Zhao, Y.; Zhu, W.; Wei, P.; Fang, P.; Zhang, X.; Yan, N.; Liu, W.; Zhao, H.; Wu, Q. Classification of Zambian Grasslands Using Random Forest Feature Importance Selection during the Optimal Phenological Period. *Ecol Indic* **2022**, *135*, doi:10.1016/j.ecolind.2021.108529.
37. Lindsay, E.; Frauenfelder, R.; Rüther, D.; Nava, L.; Rubensdotter, L.; Strout, J.; Nordal, S. Multi-Temporal Satellite Image Composites in Google Earth Engine for Improved Landslide Visibility: A Case Study of a Glacial Landscape. *Remote Sens (Basel)* **2022**, *14*, doi:10.3390/rs14102301.
38. Sellami, E.M.; Rhinane, H. A NEW APPROACH FOR MAPPING LAND USE / LAND COVER USING GOOGLE EARTH ENGINE: A COMPARISON OF COMPOSITION IMAGES. In Proceedings of the International Archives of the Photogrammetry, Remote Sensing and Spatial Information Sciences - ISPRS Archives; International Society for Photogrammetry and Remote Sensing, February 6 2023; Vol. 48, pp. 343–349.
39. Noi Phan, T.; Kuch, V.; Lehnert, L.W. Land Cover Classification Using Google Earth Engine and Random Forest Classifier-the Role of Image Composition. *Remote Sens (Basel)* **2020**, *12*, doi:10.3390/RS12152411.
40. Tsai, Y.H.; Stow, D.; Chen, H.L.; Lewison, R.; An, L.; Shi, L. Mapping Vegetation and Land Use Types in Fanjingshan National Nature Reserve Using Google Earth Engine. *Remote Sens (Basel)* **2018**, *10*, doi:10.3390/rs10060927.
41. Francini, S.; Hermosilla, T.; Coops, N.C.; Wulder, M.A.; White, J.C.; Chirici, G. An Assessment Approach for Pixel-Based Image Composites. *ISPRS Journal of Photogrammetry and Remote Sensing* **2023**, *202*, 1–12, doi:10.1016/j.isprsjprs.2023.06.002.
42. Ruefenacht, B. Comparison of Three Landsat TM Compositing Methods: A Case Study Using Modeled Tree Canopy Cover. *Photogramm Eng Remote Sensing* **2016**, *82*, 199–211, doi:10.14358/PERS.82.3.199.
43. Van Doninck, J.; Tuomisto, H. Influence of Compositing Criterion and Data Availability on Pixel-Based Landsat TM/ETM+ Image Compositing over Amazonian Forests. *IEEE J Sel Top Appl Earth Obs Remote Sens* **2017**, *10*, 857–867, doi:10.1109/JSTARS.2016.2619695.
44. JICA Cambodia Reconnaissance Survey Digital Data Project; Phnom Penh, Cambodia, 2003;
45. Congalton, R.G.; Green, K. *Assessing the Accuracy of Remotely Sensed Data: Principals and Practices*; Third Edit.; CRC Press: Boca, Raton, FL, 2019;
46. European Space Agency (ESA) Product User Manual Document Ref: WorldCover_PUM_v1.0; 2021;
47. Chandra, N.; Vaidya, H. Building Detection Methods from Remotely Sensed Images;
48. Open Street Map Roads of Cambodia Available online: https://data.opendevelopmentcambodia.net/en/dataset/road-and-railway-networks--in-cambodia (accessed on 28 May 2024).

49. Pekel, J.F.; Cottam, A.; Gorelick, N.; Belward, A.S. High-Resolution Mapping of Global Surface Water and Its Long-Term Changes. *Nature* **2016**, *540*, 418–422, doi:10.1038/nature20584.
50. Breiman, L. Random Forests. *Mach Learn* **2001**, *45*, 5–32.
51. Pal, M.; Mather, P.M. Support Vector Machines for Classification in Remote Sensing. *Int J Remote Sens* **2005**, *26*, 1007–1011, doi:10.1080/01431160512331314083.
52. Jarvis, A.; Reuter, H.I.; Nelson, A.; Guevara, E. SRTM Digital Elevation Data Version 4 Available online: https://srtm.csi.cgiar.org (accessed on 28 May 2024).
53. Asokan, A.; Anitha, J. Change Detection Techniques for Remote Sensing Applications: A Survey. *Earth Sci Inform* 2019.
54. Broge, N.H.; Leblanc, E. Comparing Prediction Power and Stability of Broadband and Hyperspectral Vegetation Indices for Estimation of Green Leaf Area Index and Canopy Chlorophyll Density. *Remote Sens Environ* **2001**, *76*, 156–172, doi:10.1016/S0034-4257(00)00197-8.
55. Dotzler, S.; Hill, J.; Buddenbaum, H.; Stoffels, J. The Potential of EnMAP and Sentinel-2 Data for Detecting Drought Stress Phenomena in Deciduous Forest Communities. *Remote Sens (Basel)* **2015**, *7*, 14227–14258, doi:10.3390/rs71014227.
56. Masek, J.G.; Vermote, E.F.; Saleous, N.E.; Wolfe, R.; Hall, F.G.; Huemmrich, K.F.; Gao, F.; Kutler, J.; Lim, T.K. A Landsat Surface Reflectance Dataset for North America, 1990-2000. *IEEE Geoscience and Remote Sensing Letters* **2006**, *3*, 68–72, doi:10.1109/LGRS.2005.857030.
57. Vermote, E.; Justice, C.; Claverie, M.; Franch, B. Preliminary Analysis of the Performance of the Landsat 8/OLI Land Surface Reflectance Product. *Remote Sens Environ* **2016**, *185*, 46–56, doi:10.1016/j.rse.2016.04.008.
58. Sesnie, S.E.; Gessler, P.E.; Finegan, B.; Thessler, S. Integrating Landsat TM and SRTM-DEM Derived Variables with Decision Trees for Habitat Classification and Change Detection in Complex Neotropical Environments. *Remote Sens Environ* **2008**, *112*, 2145–2159, doi:10.1016/j.rse.2007.08.025.
59. Shen, X.; Cao, L. Tree-Species Classification in Subtropical Forests Using Airborne Hyperspectral and LiDAR Data. *Remote Sens (Basel)* **2017**, *9*, doi:10.3390/rs9111180.
60. Belgiu, M.; Drăgu, L. Random Forest in Remote Sensing: A Review of Applications and Future Directions. *ISPRS Journal of Photogrammetry and Remote Sensing* 2016, *114*, 24–31.
61. Fraser, B.T.; Congalton, R.G. Monitoring Fine-scale Forest Health Using Unmanned Aerial Systems (UAS) Multispectral Models. *Remote Sens (Basel)* **2021**, *13*, doi:10.3390/rs13234873.
62. Lin, X.; Chen, J.; Lou, P.; Yi, S.; Qin, Y.; You, H.; Han, X. Improving the Estimation of Alpine Grassland Fractional Vegetation Cover Using Optimized Algorithms and Multi-Dimensional Features. *Plant Methods* **2021**, *17*, 1–18, doi:10.1186/s13007-021-00796-5.
63. Blaschke, T. Object Based Image Analysis for Remote Sensing. *ISPRS Journal of Photogrammetry and Remote Sensing* **2010**, *65*, 2–16.
64. Robertson, L.D.; King, D.J. Comparison of Pixel-and Object-Based Classification in Land Cover Change Mapping. *Int J Remote Sens* **2011**, *32*, 1505–1529, doi:10.1080/01431160903571791.
65. Foody, G.M. Status of Land Cover Classification Accuracy Assessment. *Remote Sens Environ* **2002**, *80*, 185–201, doi:10.1016/S0034-4257(01)00295-4.
66. Congalton, R.G. A Review of Assessing the Accuracy of Classifications of Remotely Sensed Data. *Remote Sens Environ* **1991**, *37*, 35–46, doi:10.1016/0034-4257(91)90048-B.
67. Congalton, R.G.; Green, K. A Practical Look at the Sources of Confusion in Error Matrix Generation. *Photogramm Eng Remote Sensing* **1993**, *59*, 641–644.
68. Olofsson, P.; Foody, G.M.; Stehman, S. V.; Woodcock, C.E. Making Better Use of Accuracy Data in Land Change Studies: Estimating Accuracy and Area and Quantifying Uncertainty Using Stratified Estimation. *Remote Sens Environ* **2013**, *129*, 122–131, doi:10.1016/j.rse.2012.10.031.
69. Chapin III, F.S.; Zavaleta, E.S.; Eviner, V.T.; Naylor, R.L.; Vitousek, P.M.; Reynolds, H.L.; Hooper, D.U.; Lavorel, S.; Sala, O.E.; Hobbie, S.E.; et al. Consequences of Changing Biodiversity. *Nature* **2000**, *405*, 234–242, doi:10.1038/35012241.
70. Vitousek, P.M. Beyond {Global} {Warming}: {Ecology} and {Global} {Change}. *Ecology* **1994**, *75*, 1861–1876, doi:10.2307/1941591.
71. Packman, C.E.; Gray, T.N.E.; Collar, N.J.; Evans, T.D.; Van Zalinge, R.N.; Virak, S.; Lovett, A.A.; Dolman, P.M. Rapid Loss of Cambodia's Grasslands. *Conservation Biology* **2013**, *27*, 245–247, doi:10.1111/cobi.12018.
72. Li, M.; Zuo, S.; Su, Y.; Zheng, X.; Wang, W.; Chen, K.; Ren, Y. An Approach Integrating Multi-Source Data with LandTrendr Algorithm for Refining Forest Recovery Detection. *Remote Sens (Basel)* **2023**, *15*, doi:10.3390/rs15102667.
73. Pasquarella, V.J.; Arévalo, P.; Bratley, K.H.; Bullock, E.L.; Gorelick, N.; Yang, Z.; Kennedy, R.E. Demystifying LandTrendr and CCDC Temporal Segmentation. *International Journal of Applied Earth Observation and Geoinformation* 2022, *110*.
74. Du, Z.; Yu, L.; Li, X.; Zhao, J.; Chen, X.; Xu, Y.; Yang, P.; Yang, J.; Peng, D.; Xue, Y.; et al. Integrating Remote Sensing Temporal Trajectory and Survey Statistics to Update Land Use/Land Cover Maps. *Int J Digit Earth* **2023**, *16*, 4428–4445, doi:10.1080/17538947.2023.2274422.

 doi:10.20944/preprints202407.0174.v1

75. Wu, J.; Jin, S.; Zhu, G.; Guo, J. Monitoring of Cropland Abandonment Based on Long Time Series Remote Sensing Data: A Case Study of Fujian Province, China. *Agronomy* **2023**, *13*, doi:10.3390/agronomy13061585.
76. Zhu, Z.; Woodcock, C.E. Continuous Change Detection and Classification of Land Cover Using All Available Landsat Data. *Remote Sens Environ* **2014**, *144*, 152–171, doi:10.1016/j.rse.2014.01.011.
77. Lillesand, T.; Kiefer, R.W.; Chipman, J. *Remote Sensing and Image Interpretation*; 7th ed.; John Wiley and Sons Ltd.: USA, 2015; ISBN 978-1-118-34328-9.
78. Jaroci'nska, A.J.; De Jong, S.M.; Schaepman, M. Remote Sensing and Digital Image Processing Volume 20 EARSeL Series Editor;
79. Hor, S.; Saizen, I.; Tsutsumida, N.; Watanabe, T.; Kobayashi, S. The Impact of Agricultural Expansion on Forest Cover in Ratanakiri Province, Cambodia. *Journal of Agricultural Science* **2014**, *6*, doi:10.5539/jas.v6n9p46.
80. Song, S.; Lim, P.; Meas, O.; Mao, N. The Agricultural Land Use Situation on the Periphery of the Tonle Sap Lake. *International Journal of Environmental and Rural Development* **2011**, *2*, 66–71.
81. Tamiminia, H.; Salehi, B.; Mahdianpari, M.; Quackenbush, L.; Adeli, S.; Brisco, B. Google Earth Engine for Geo-Big Data Applications: A Meta-Analysis and Systematic Review. *ISPRS Journal of Photogrammetry and Remote Sensing* **2020**, *164*, 152–170, doi:10.1016/j.isprsjprs.2020.04.001.